Lunar Microgrid Trade Studies to Define Interface Converter Requirements

George Thomas[1], Matthew Granger[2], and Jeffrey Csank[3]
NASA Glenn Research Center, Cleveland, OH, 44135, USA

The National Aeronautics and Space Administration (NASA) is interested in developing an incremental lunar power grid to support continuous human/robotic operations under the Artemis missions and can scale to global power utilization and industrial power levels. The initial lunar surface power system will be composed primarily of assets that contain their own power generation and energy storage. These assets can be connected to form a grid, which allows power to be shared between the system's distributed energy resources. This grid can provide backup power to existing assets as well as primary power to future assets. A trade study was conducted for an Artemis scale grid, which has identified 3 kVAC as an ideal transmission voltage. This paper documents the analysis and findings from these trade studies. These studies were used to define the operating voltage and develop a common interface for connecting lunar surface assets to the power grid. The Universal Modular Interface Converter (UMIC) connects lunar surface assets to the high voltage grid. Products from this grid definition and UMIC development work will enable highly reliable and available power for Artemis and future planetary surface missions, which is key to achieving NASA's long-term vision of space exploration.

I. Introduction

NASA's Artemis missions seek to establish a permanent presence on the lunar surface including manned operations [1]. A primary goal of the Artemis missions is to develop and demonstrate technologies required for the Mission to Mars in a relevant environment as close to the Earth as possible. NASA plans to demonstrate multiple technologies on the lunar surface, including in-situ resource utilization (ISRU), fission surface power (FSP), surface habitat and others. Current plans dictate that each asset will include its own power source and energy storage devices because they will be launched independently and thus must be able to operate independently.

There are significant benefits to establishing a power grid for Artemis by connecting these assets. First, the grid will increase the reliability and availability of electric power to Artemis loads and reduce overall mission risk. It can do this because it will allow Artemis assets to share excess power and provide backup power to high priority loads on the grid (e.g., the habitat when a human crew is present). It will also enable new assets to be deployed that do not carry their own power. This capability will facilitate future lunar missions beyond Artemis and help enable NASA's vision for a commercial lunar economy.

Multiple papers have been published analyzing possible lunar grids. Ref. [2] documents cable-focused DC power transmission trades for a lunar surface power system, with powers up to 800 kW and distances up to 5 km. A detailed cable model is described in this work, including electrical and thermal models, and multiple cable configurations are compared (suspended above ground vs buried, two-wire vs coaxial, etc.). This paper makes recommendations about which configuration is best for different scenarios. Ref. [3] presents 100 m to 10 km transmission of power up to 50 kW, using DC and AC cables, RF, and laser power beaming. The main conclusion is that that DC cables are predicted to be the mass optimal transmission method for this application, followed closely by AC cables. Ref [4] compares DC cables to multiple power beaming methods (RF, laser, and a light bender concept based on mirrors, lenses, and solar arrays) for powers up to 50 kW and distance up to 15 km. A fair level of detail is given towards the sizing of components and associated model equations. This work suggests that DC cables are mass optimal for shorter distance

[1] Electrical Engineer, Power Management and Distribution Branch, AIAA Member
[2] Electrical Engineer, Power Management and Distribution Branch
[3] Electrical Engineer, Power Management and Distribution Branch, AIAA Senior Member

power transmission (3-5 km), whereas optical power transmission is mass optimal for longer distances. It also suggests that optical power transmission is more flexible in terms of operations. Ref. [5] conducted an end-to-end conceptual design of a lunar base including in-situ resource utilization and a habitat. This work included detail on sizing and mass models of cables, power generation and storage elements (solar arrays, batteries or regenerative fuel cells [RFCs], and fission power), cables, and converters or battery charge controllers. This work does not focus on power transmission but does present some design values chosen for relevant variables (e.g., 1.5 kVDC transmission from the fission plant to the habitat).

The NASA Science Technology Mission Directorate (STMD) Game Changing Development (GCD) program's Microgrid Definition and Interface Converter for Planetary Surface (MIPS) project started with an initial goal to define parameters for a proposed Artemis scale lunar grid via analytical design trade studies. These lunar grid studies were conducted in two parts. First, a point-to-point transmission study was conducted to narrow down the solution space and serve as a platform for maturing the analysis tools for the studies. Then, full grid studies were conducted for final selection of grid parameters. This paper presents these full grid studies and associated results. Section II describes the modeling approach and assumptions made in this work. Section III describes the final grid studies. Finally, Section IV presents conclusions drawn from the data.

II. Models and Assumptions

The lunar grid trade studies were conducted using the Electrical Power System—Sizing and Analysis Tool (EPS-SAT) [6] [7]. EPS-SAT is an object oriented, MATLAB-based tool for system level analysis of electrical power systems. Power system models can be created by writing a MATLAB code file that instantiates and connects power components to build up an architecture. Parameters such as voltages, currents, and efficiencies are taken as inputs or solved for by a Newton-Raphson solver, which varies any independent variables it is given until all dependent variables converge (these are typically statements of conservation laws such as Kirchoff's voltage and current laws).

This work studies a notional Artemis scale lunar grid, as shown in Fig. 1.

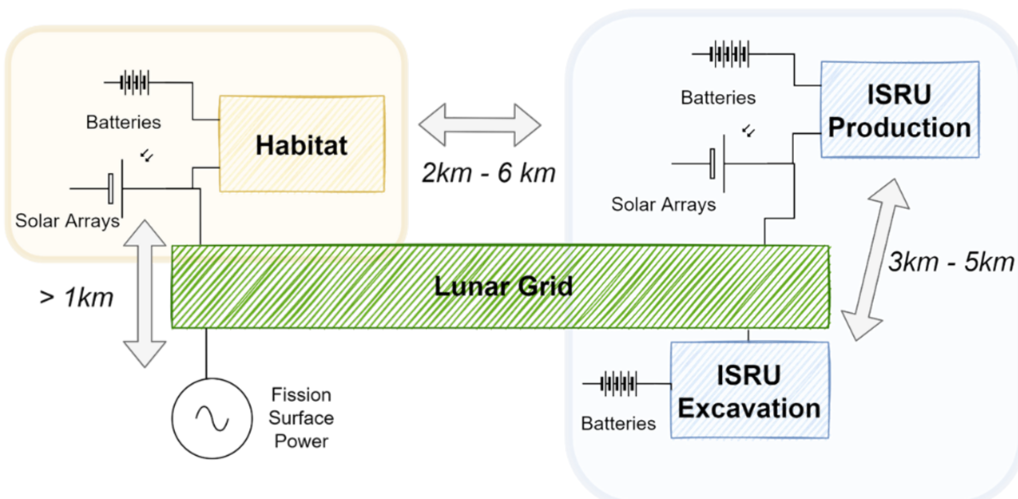

Fig. 1 Artemis lunar grid notional diagram.

This grid includes a habitat microgrid shown with a yellow background, an ISRU microgrid shown in a blue background, and an overall lunar grid connecting them in green. Details about the models and assumptions used in the analytical EPS-SAT studies of this system are given in this section. Subsections A and B describe detailed cable and converter models developed for this work, based off previous models developed for NASA. Subsection C lists assumptions of where Artemis sites will be located, which drives the transmission distance assumptions used in the models. Finally, Subsection D lists assumptions associated with loads and sources in the Artemis power system.

A. Power Transmission: Lunar Cables

These trade studies assume that a cable will be used to transmit power on the lunar surface. To capture cable design trends in the EPS-SAT tool, a lunar surface cable model was created based on the model presented in Ref [2]. This model captures a variety of design variables, including the following:

- Design efficiency (at maximum power)
- Height above ground of the cable installation (positive numbers represent height suspended above surface, zero represents cables laying on surface, and negative represents cables buried at a depth below surface)
- Length of the cable
- Number of parallel conductors per phase
- Insulation safety factor (cable insulation thickness is sized to this factor of the material breakdown V/mm)
- Cable conductor and insulation materials (copper/aluminum, and PTFE/ETFE/uninsulated)

The tool will allow the cable voltage, current, electrical power type (DC, 3-phase AC, single-phase AC) and frequency to be sized to arbitrary input conditions.

The cable wire gauge is selected as the lightest wire gauge that meets or exceeds the design efficiency, bounded by upper and lower wire gauge limits set by the user. If a single wire within the gauge limits does not meet the efficiency target, multiple parallel wires within the limits will be used. The wire insulation thickness is sized to operate with a voltage gradient no greater than the insulation safety factor times the insulation material breakdown (V/mm), assuming the cables are touching. The cable resistance is based on Ohm's law with resistivity equal to the conductor resistivity corrected for the conductor temperature, and with skin effect and proximity effect applied. Cable inductance is calculated using standard equations based on the geometric mean radius of each phase conductor (or parallel bundle of phase conductors) and geometric mean distance between conductors or parallel bundles [8]. It is assumed that individual conductors are twisted and bundled tightly to minimize inductance. Skin and proximity effects are accounted for by adjusting the AC resistance (if the cable carries AC) using published approximations [9]. Cable design parameter assumptions used in this work are given in Table 1.

Table 1 Cable design assumptions for grid trade studies.

Parameter	Value
Design Efficiency	90% at 40 kW power transmission
Installation Location	On lunar surface
Cable Length	2-5 km based on site selection data
Wire Gauges Allowed	10 – 14 AWG
Number of Parallel Phase Conductors	Varied to achieve allowed wire gauges
Insulation Safety Factor	10x
Conductor Material	Copper
Insulation Material	ETFE (Tefzel)

One item neglected from the model is inductive coupling between cables laid on the surface and regolith. This was neglected due to the lack of published data on this effect. Previous unpublished NASA studies estimated prohibitive levels of losses (above 10%) due to power inductively coupled into and dissipated in the regolith if 60 Hz power cables were laid on the surface. However, these studies estimated more reasonable, low single digit percentage losses if 400 Hz cables are laid on the surface. These facts suggest that 400 Hz and greater frequencies may be best for power transmission using cables laid on the lunar surface, however future work should include validation of this data. Another item neglected from cabling is armor, abradable sheathing or jacket materials, or possible fillers or structural members within the cable. These were neglected because the final construction approach of lunar surface cables has not been decided. It is recommended that if using any cable data from this paper, that users apply mass fractions to the data corresponding with any assumptions they want to make regarding these additional cable elements.
.

B. Power Management: Converters

Converters are needed to convert grid power (assumed to be in the kilovolt range and could be AC or DC) to the native power type used at loads and sources (tens to hundreds of volts DC). It is assumed that these grid interface converters are bidirectional so that they can transmit power from any one asset that has excess power to another asset that has a deficit. A major goal of these grid trade studies is to define the parameters of the grid, such that these can drive the design requirements for a NASA reference converter.

For these studies a generalized converter model was developed in the EPS-SAT environment. Due to the need to analyze all possibilities for power transmission topologies, the EPS-SAT converter model can convert electrical power between any configuration (AC or DC to AC or DC, boost or buck). The converter model takes efficiency, topology (AC/DC), frequency, and output voltage as parameters. Values assumed for any variables not varied during the trade study are given in Table 2. The converter operates as an isolated, regulating converter, maintaining voltage and frequency setpoints at its output. A design efficiency input parameter is used by the model to produce a power loss for that component in EPS-SAT. Mass is calculated using a model based on Ref. [10]. The AC variations of the converter are also capable of power factor correction.

Table 2 Converter design assumptions for grid trade studies.

Parameter	Value
Design efficiency if a DC/DC converter	95%
Design efficiency if a DC/AC converter	96.5%
Design efficiency if an AC/AC converter with no frequency change (a transformer)	98%
Design efficiency if an AC/AC converter with frequency change (a full AC/AC converter)	95%

It is assumed that the maximum DC grid voltage achievable with flight parts at high reliability is 1.5 kV, and that there is no similar limitation on AC grid voltage. Bidirectional DC/DC converter output voltages above 300 VDC require a number of series stacked stages since presently available power switches enable roughly 300 VDC per series stage (after de-rating for radiation). As designs include a higher number of series stages, the overall design reliability decreases. It is assumed that more than four or five series stages results in a prohibitively high reliability risk. Note that this risk can be mitigated if the individual stages are designed to fail such that the stack can continue to operate within specifications. This should be possible but has not proven in a flight design. Thus, it is considered prohibitive at present to design a high reliability DC-DC converter with high side voltage above 1.5 kV. However, the trade studies in this work examine DC grid voltages above this value to show what is possible if higher voltage, space rated parts become available.

C. Site Selection Assumptions

NASA is considering multiple sites at the Lunar south pole for its Artemis missions [11]. This work assumes the Artemis power system will be distributed along the Shackleton crater rim and into the Shackleton-de Gerlache connecting ridge because of its proximity to the south pole, favorable terrain, and access to sunlight. Based on this, further assumptions about placement of assets are made to evaluate possible grid architectures, and these assumptions are made to be consistent with plans and constraints for loads and sources such as ISRU and FSP. There are two main objectives to consider, i) placing lunar assets to maximize sunlight availability, both in continuous days of sunlight and amount of total yearly hours of sun, and ii) placing assets as close as possible to each other to minimize transmission losses. Other minor objectives include how extensible the power system is (ease of extending the grid with additional assets in the future), and the proximity of grid assets to other locations where Artemis operations will be conducted (exploration of craters, etc.).

Shackleton crater is a large crater at the lunar south pole. The crater itself is approximately 2 miles deep and more than 12 miles wide. Since the crater is located at the southern pole and the moon has a very small tilt, the inside of the crater is permanently shadowed. The temperature inside the crater has a yearly average of 90 K and never exceeds 100 K [12] [13]. The cold temperature and lack of sunlight make this crater ideal for obtaining lunar regolith with very high water-ice concentration. For determining a relative distance, the ISRU Mining site is placed in the closest Permanently Shadowed Region (PSR) outside of Shackleton crater. The ISRU Production site (the largest producer and consumer of power) would be located on the rim to maximize sunlight availability. Finally, the Habitat will be placed further from the ISRU Production site as shown in Fig. 2. The FSP plant is assumed to be located close to the Habitat as these assets are required to be connected, however, the FSP is simultaneously placed in a location where it is also close to the other assets, to enable its power to most easily be dispatched to any loads as needed. Based on this layout, the various distances between sites are shown in Table 3.

Table 3 Distance between lunar assets for lunar base located on the rim of Shackleton Crater

Distance (km)	Habitat	FSP	ISRU Production	ISRU Mining
Habitat		2.6	3.4	3.2
FSP	2.6		3.1	3.0
ISRU Production	3.4	3.1		3.6
ISRU Mining	3.2	3.0	3.6	

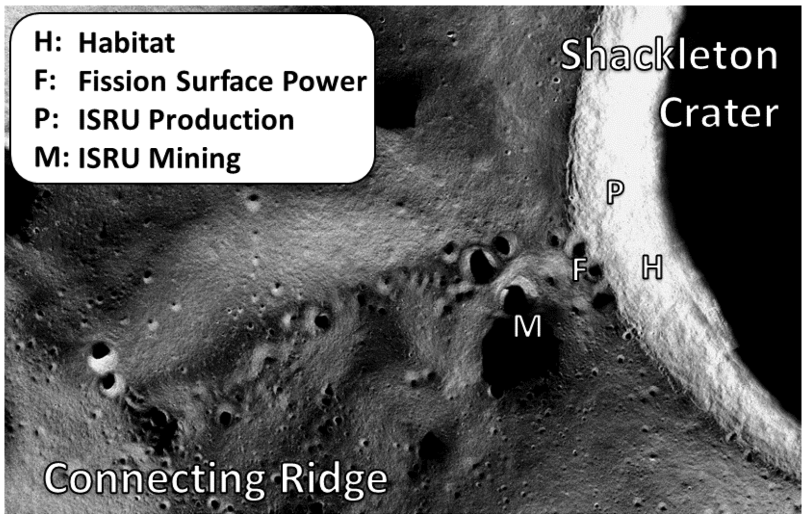

Fig. 2 Diagram of lunar base around Shackleton Crater rim.

D. Load and Source Assumptions

The Artemis power system as shown in Fig. 1 has four asset locations, the Habitat (H), FSP (F), ISRU Mining (M), and ISRU Production (P). It is assumed that three of these assets are sources or contain sources (Habitat, FSP, and ISRU Production) and three have loads (Habitat, ISRU Mining, and ISRU Production). Further, all sources except for FSP are assumed to be DC and based on solar arrays with batteries. Solar arrays for the lunar power system are assumed to be vertically deployed and each one is assumed capable of more than 10 kW peak power at end of life, consistent with requirements for NASA's vertical solar array technology (VSAT) project. It is assumed that the habitat has peak loading equal to 20 kW, and thus has two solar arrays for a total power capability just above 20 kW and capable of meeting habitat peak loading needs. The FSP plant is assumed to be sized to deliver 40 kW to the Habitat, to be consistent with NASA's FSP project. The ISRU loading requirements are assumed to be 90 kW total, with 22 kW required at the mining site, and 68 kW required at the production site. The ISRU Production site is assumed to include seven solar array installations for a total source capability of 70 kW. These power value assumptions are summarized in Table 4.

Table 4 Assumed source and load power capabilities of Artemis lunar power system assets.

Capability	Asset	Value
Source Power	Habitat	20 kW
	FSP	40 kW
	ISRU Production	70 kW
Load Power	Habitat	20 kW
	ISRU Production	68 kW
	ISRU Mining	22 kW

III. Grid Trade Studies

Subsection A within this section covers grid studies that were used to select the parameters for the proposed Artemis grid. Subsection B covers studies investigating a hypothetical expansion of the lunar grid from Artemis scale to add initial in-space manufacturing, a space-manufactured solar array installation, and a second commercial habitat.

A. Artemis Grid Trade Studies

The studies were conducted using the assumptions and inputs given in Section II. A list of parameters varied over the course of the study is given in Table 5.

Table 5 Grid study sweep parameters.

Variable	Values Used
Power Type	DC vs 3-Phase AC
Voltage	1.2, 1.5, 2.4, 3.0, 4.5, and 6.0 kV line-to-line
Frequency	60, 400, 800, and 1000 Hz

The grid architecture was also varied in this work. Three possible architectures were evaluated, including radial, ring, and mesh. A diagram showing these architectures is shown in Fig. 3.

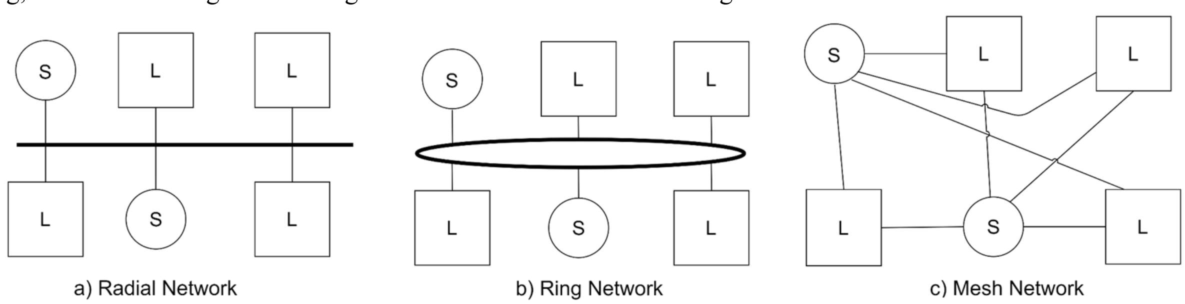

Fig. 3 Generalized radial network (a), ring network (b), and mesh network (c).

All possible permutations of the design variables in Table 5 were sized for each type of grid architecture found in Fig. 3. Note that in this study all designs are sized to approximately the same point-to-point transmission efficiency. This allows design solutions to be easily compared by total transmission mass, which is the figure of merit used in this work. Total transmission system mass is calculated by summing the masses of each converter and cable in the system. Not included are the masses for any equipment needed to deploy the transmission system. Fig. 4 shows the transmission mass vs voltage for all designs considered for the radial network. It should be noted that the masses of these transmission system designs are all dominated by cable weight, as shown in Fig. 5.

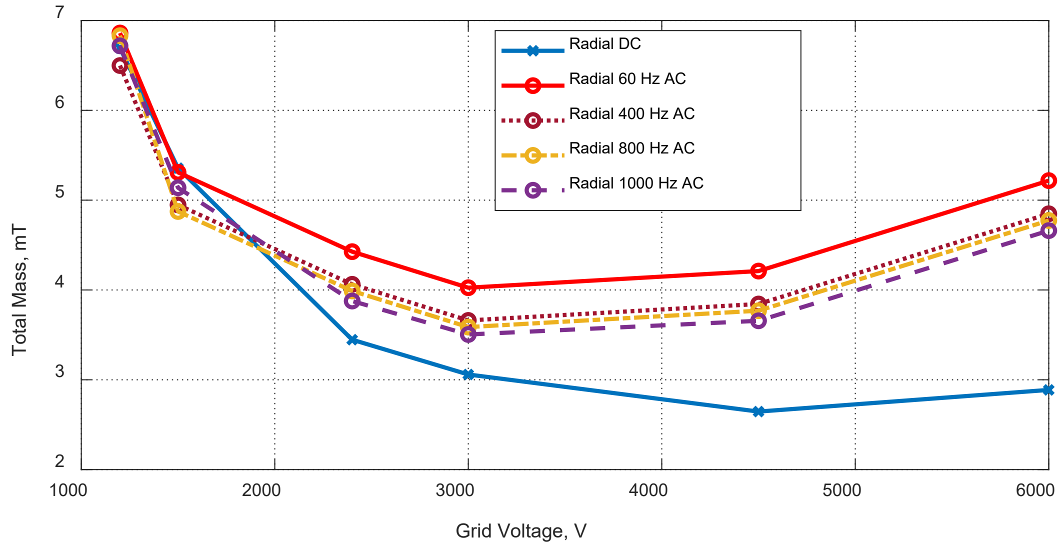

Fig. 4 Radial power system mass vs voltage.

This data shows the mass vs voltage trend for DC designs in blue and AC designs with the remaining colors. All designs show minimum mass solutions at an intermediate voltage between the 1.2 and 6 kV search limits. The minimum mass solution for DC designs is at 4.5 kV and for AC designs is at 3 kV regardless of the selected line frequency. AC designs reach their minimum mass at lower voltage than DC because AC cable designs have heavier insulation than DC designs. This is because AC conductors must be sized to a peak voltage value of √2 times the rated RMS value, whereas DC conductors need only be sized to the DC value which is the same as the rated RMS value. Also, AC conductors are smaller for the same power carrying capability (the same conductor material is distributed among three-phase conductors vs two DC conductors [hot and return])—these smaller wires mean more total surface area that must be insulated. As a result, AC cable insulation designs get heavier with voltage more quickly than DC designs, and the impact of this difference is significant to total transmission mass because transmission mass is dominated by cable mass. Mass also decreases in AC designs as frequency is increased due the fact that the higher frequency magnetics in the converters can be miniaturized, however does not significantly affect total transmission mass due to the fact that the transmission mass is dominated by cable mass. Overall, the data shows that DC designs tend to have lower mass than AC, and that the minimum mass solution for DC designs is at higher voltages than AC.

Detailed transmission system mass stacks for the mass optimal 4.5 kVDC and 3 kVAC solutions are given are given in Fig. 5, along with the 1.2 kVDC solution which is assumed to be the highest DC grid voltage achievable at high reliability given currently available space-rated power switches.

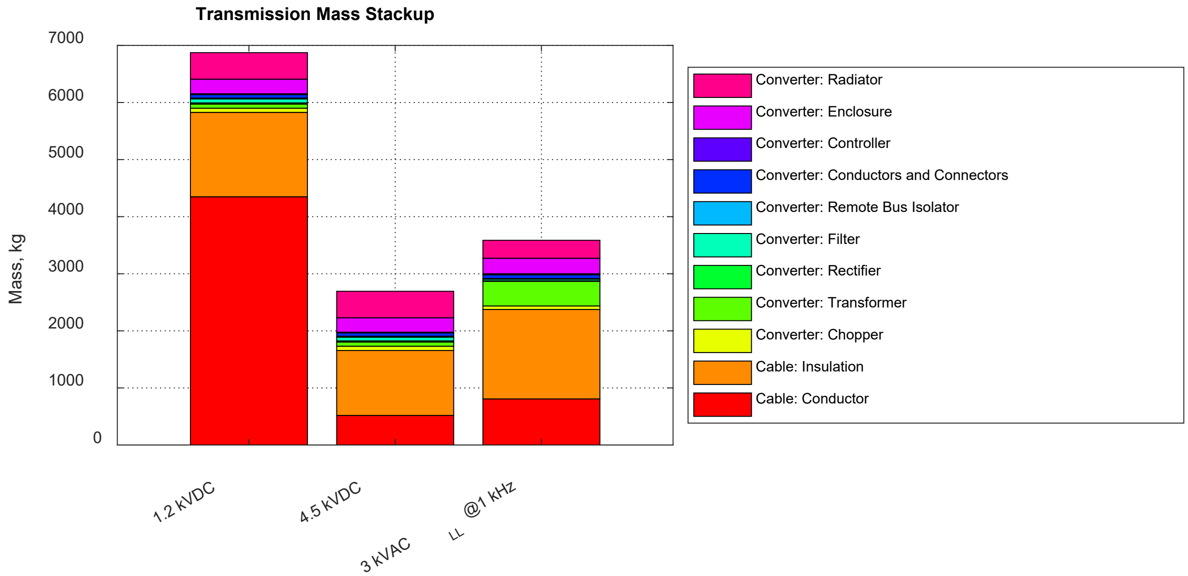

Fig. 5 Total transmission mass stackup chart for 1.2 kVDC, 4.5 kVDC, and 3 kVAC radial grid design solutions.

This graphic clearly shows that transmission mass is dominated by cable mass, with higher voltage solutions having lower overall cable mass than lower voltage ones. Assuming that the 4.5 kVDC solution is not feasible, the optimal solution is 3 kVAC. At the scale shown in this figure, the only significant difference between these solutions in terms of cable mass is that the AC solution has a much larger transformer mass than the DC solutions. In order to see converter mass differences more clearly, mass stack data showing only the converters (omitting the cables) are given in Fig. 6.

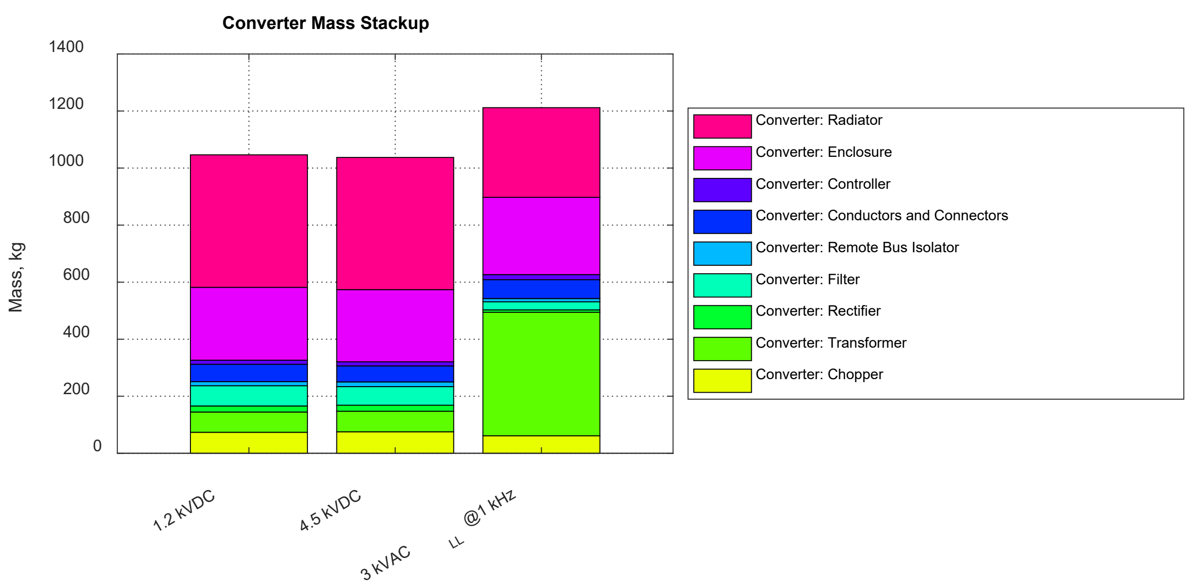

Fig. 6 Converter mass stackup charts for 1.2 kVDC, 4.5 kVDC, and 3 kVAC radial grid design solutions.

At this scale, one can also see that the DC solutions have lower converter mass than the AC solution. This is driven primarily by the higher transformer mass in the AC solution, given that the AC transformer is assumed to be sized to line frequency, whereas the DC transformers are assumed to be sized to the DC/DC converter internal switching frequency, which is assumed to be 50 kHz. Also of note is that the DC solution converters show higher filter mass than the AC solution ones. This is primarily driven by an assumption that the DC system converter needs a relatively large filter to achieve reasonable ripple, whereas AC system converter ripple is at least partially attenuated by the transformer, resulting in a lesser need for large discrete filter components.

The next system studied was the ring architecture. Note that mass stack trends for this system are similar to the trends seen with the radial grid and thus aren't shown. The mass vs voltage data for the ring system are shown in Fig. 7. This data shows approximately a 50% mass increase vs the radial system for each voltage and power type. The overall trends are the same between ring and radial: one can see the same minimum mass solutions 4.5 kVDC and 3 kVAC, and same shape of the associated curves.

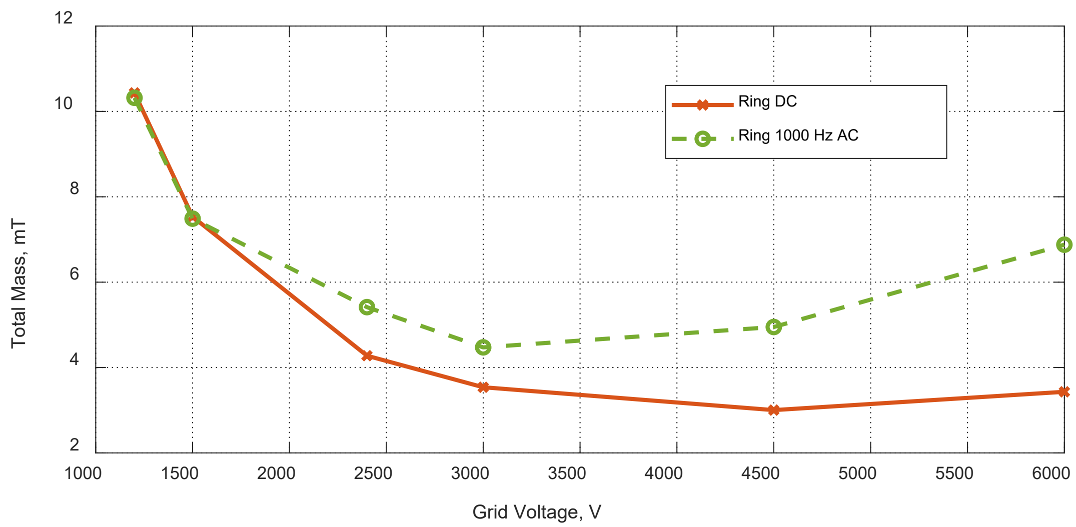

Fig. 7 Ring power system mass vs voltage.

Likewise, the mesh architecture shows similar trends to the radial and ring, with an overall approximately 75-100% increase in mass vs the radial system. The mesh architecture mass vs voltage data are shown in Fig. 8.

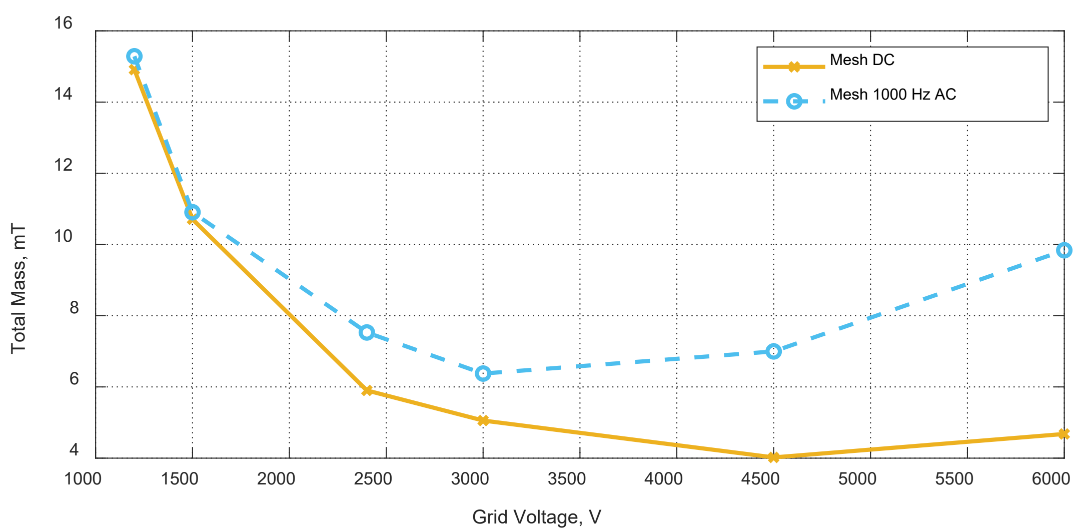

Fig. 8 Mesh power system mass vs voltage

Several conclusions about grid parameters can be drawn from this data. One is that the mass optimal feasible design solution for this Artemis scale grid is predicted to be 3 kVAC with a transmission frequency of 1 kHz. Another is that AC cable designs tend to be heavier than DC due to heavier insulation mass. AC cable insulation mass also increases more quickly with voltage than DC insulation mass does, and this causes AC grid designs to reach minimum mass at lower voltages than DC. Note that if high reliability space-rated DC/DC converter designs can be demonstrated at voltages above 2 kV, then DC may become the more mass optimal power type for Artemis scale grids.

Conclusions can be drawn regarding grid architectures as well. Adding additional lines (going from a radial system to a ring or mesh) does not change the mass vs voltage trends. The primary difference between architectures is that adding lines adds redundancy at the expense of additional mass. The optimal tradeoff between mass and redundancy will be difficult to evaluate without detailed reliability models, and these models will be difficult to construct. It is most likely that radial type architectures will be constructed first on the lunar surface with additional lines added to add reliability as needed as the grid grows.

B. Artemis Grid Expansion Studies

NASA anticipates an expansion of the Artemis power system to eventually include in-space manufacturing, a commercial lunar economy, and eventually global exploitation of lunar resources. A hypothetical scenario was considered where a higher power commercial habitat site with multiple buildings over a 2 km footprint is added, along with a 10 km scale commercial in-space manufacturing site featuring a manufacturing location and locally manufactured solar power generation. Power levels for the commercial habitat and in-space manufacturing site are assumed to be 100 kW and 1 MW respectively. A larger transmission system will be required to connect the original 3 kVAC Artemis grid and these new sites. This new transmission system will have to be sized to carry much larger amounts of power over a longer distance. Assuming the transmission system must connect multiple MW-level sites like the in-space manufacturing site, the transmission system is likely to be sized for 10 MW over 50 km distances and is depicted in in Fig. 9. Studies were conducted to select appropriate voltage levels for the larger transmission system shown in blue in Fig. 9, the in-space manufacturing power system shown in orange, and the commercial habitat in green. To simplify these studies, a constant wire gauge was used for the cabling and selected such that it is large enough to handle the associated power level without exceeding temperature limits. For each study, a point-to-point transmission model was set up with the associated power level and distance and was ran with a set of different voltages. Figures are drawn showing cable losses vs distance for each voltage level evaluated, with a maximum acceptable cabling loss level of 3% shown as a red dashed line. Voltage levels that do not exceed the loss level for the specified distance are considered valid solutions. Note that it is assumed that the cables for these transmission systems would be manufactured on the lunar surface, so mass is not a significant concern. Instead of seeking to minimize mass, these studies select the lowest voltage level that meets the minimum loss criterion, because it is assumed that lower voltages pose lower infrastructural costs (smaller suspension towers, smaller keepout zones, etc).

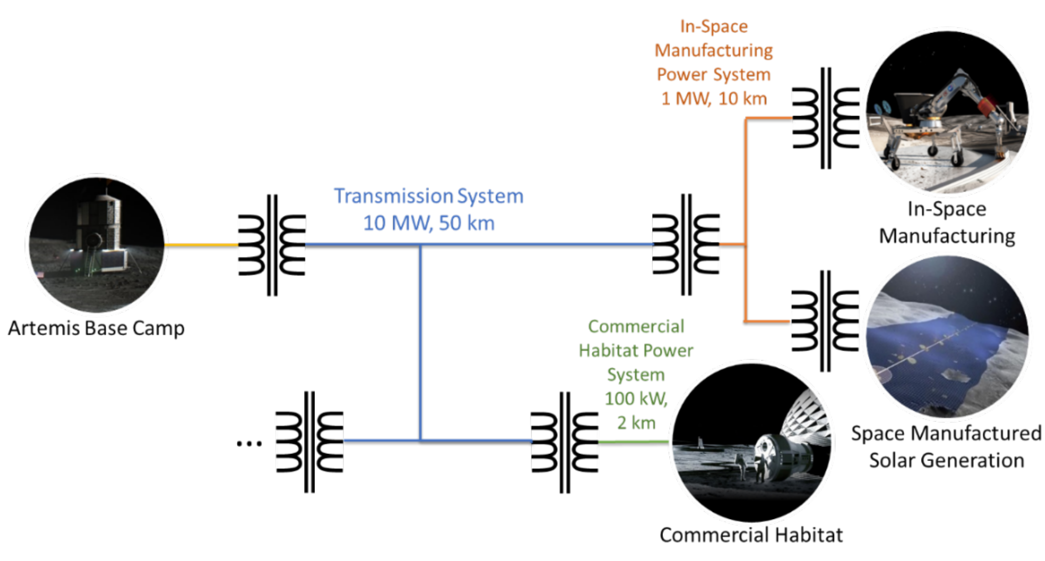

Fig. 9 Hypothetical lunar grid expansion with distances and power levels shown for different legs of the overall power system.

The commercial habitat bus was assumed to use an 8 AWG cable. Voltages between 3 and 18 kV were evaluated. The cable loss vs length data for each voltage are shown in Fig. 10. This figure shows that for the 2 km distance regime assumed, the lowest voltage tested that does not exceed the 3% cable loss constraint is 6 kV. This means that this voltage level is an appropriate one for the commercial habitat power system.

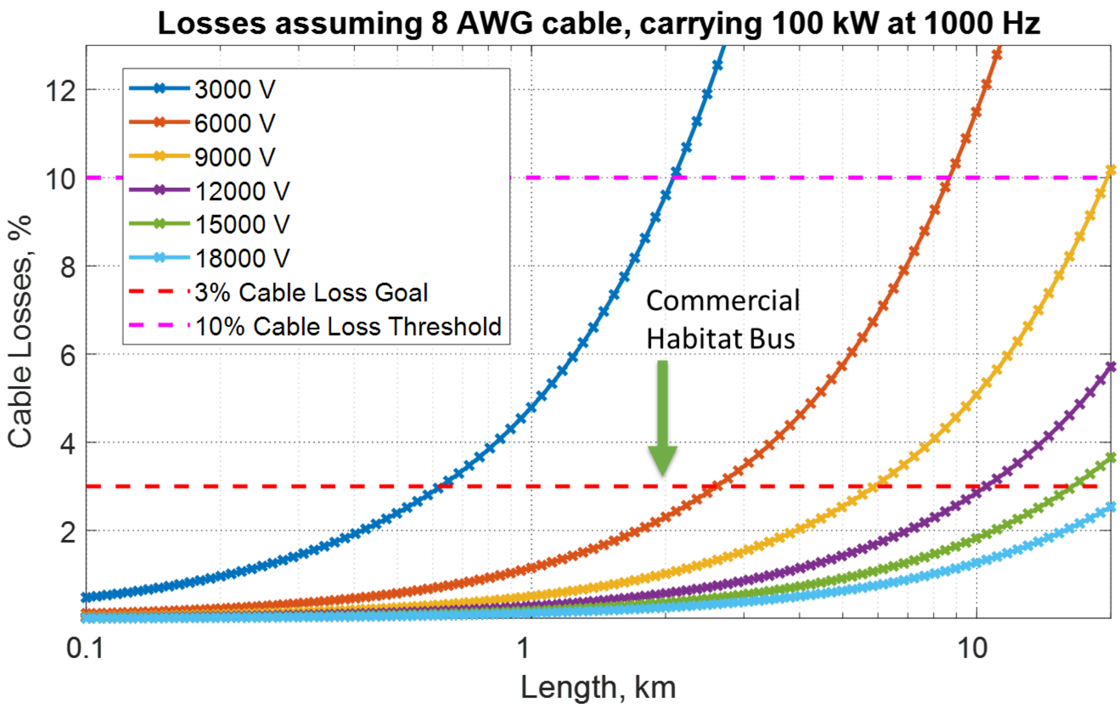

Fig. 10 Loss vs length data for the commercial habitat bus, with an arrow pointing to the design solution chosen (6 kV).

The in-space manufacturing power system was assumed to use 4 AWG cables. Voltages between 9 and 24 kV were evaluated for this system, and the associated loss vs length data are shown in Fig. 11. This figure indicates that for the 10 km distance assumed, the appropriate voltage level is 24 kV.

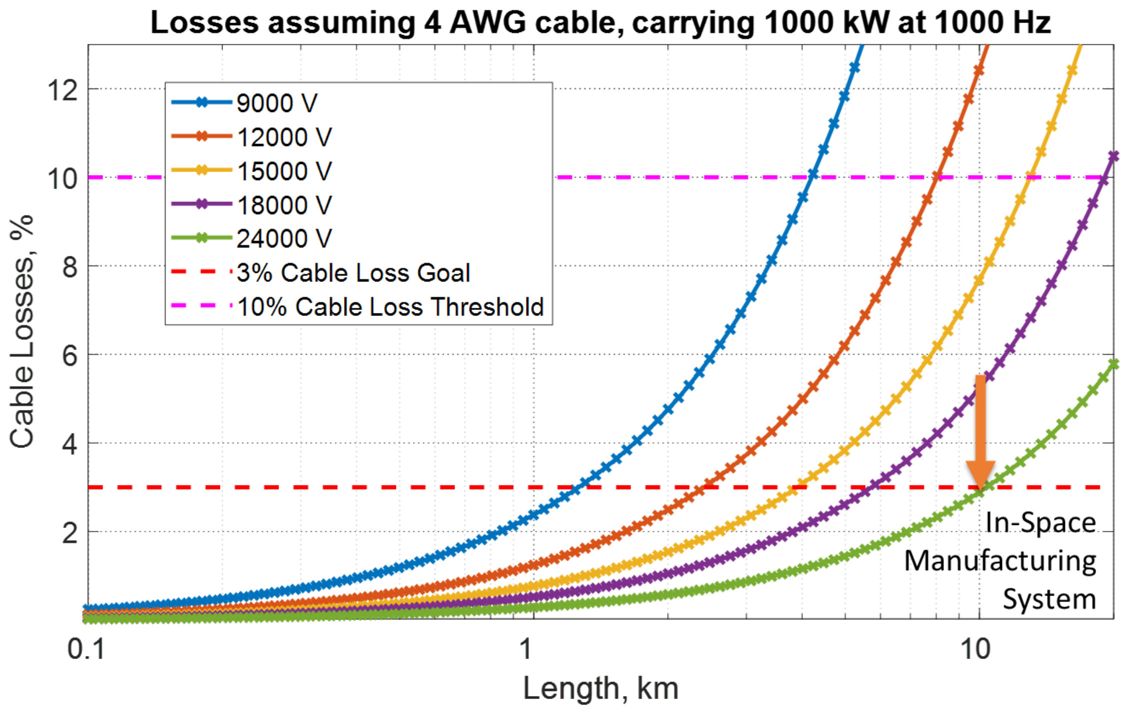

Fig. 11 Loss vs length data for the in-space manufacturing bus, with an arrow pointing to the design solution chosen (24 kV).

Finally, the high power, high distance leg of the power transmission system was studied. This system was assumed to use 4/0 AWG cables. For this system, voltages between 30 and 240 kV were evaluated. The associated loss vs length data are shown in Fig. 12. For this part of the system, the data recommend a 90 kV voltage level.

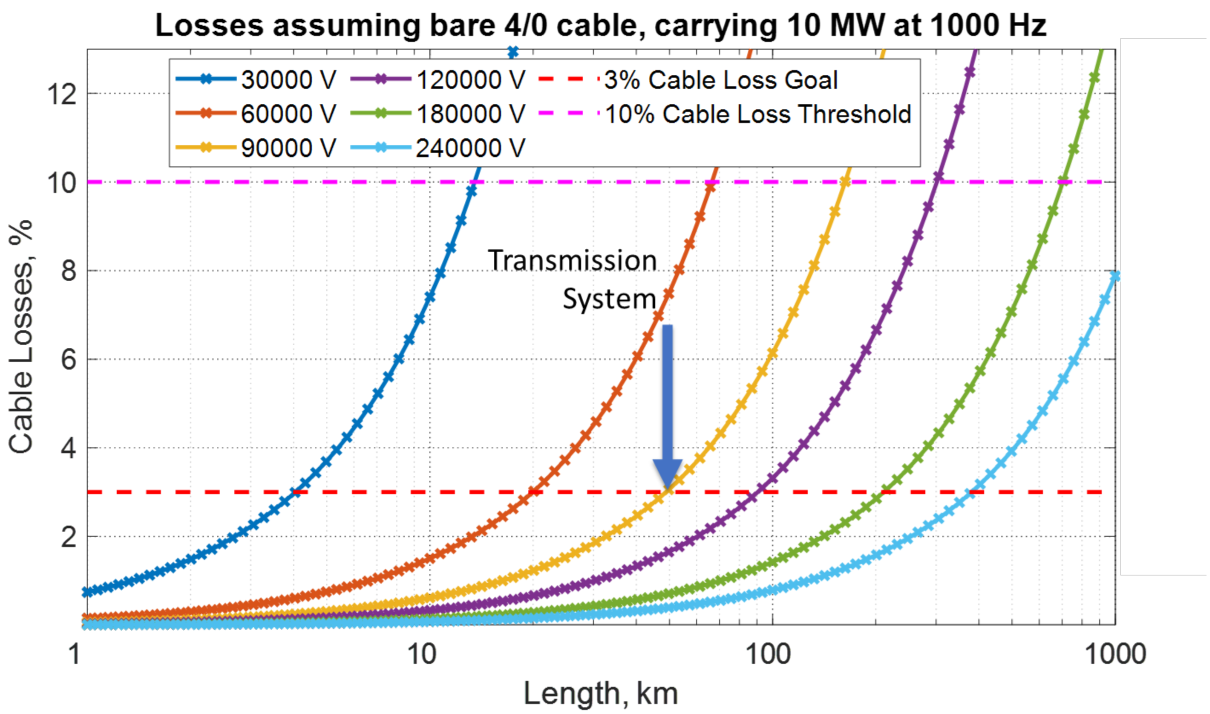

Fig. 12 Loss vs length data for the large-scale lunar transmission system, with an arrow pointing to the design solution chosen (90 kV).

Overall, the data suggest that as the lunar surface power system grows to include multiple different subsystems at different voltage and power scales, a reasonable voltage must be selected for each subsystem. The voltage chosen should match the distance and power scale reasonably well, otherwise the power system will be too lossy (if the voltage is too low), or the infrastructure will be oversized, incurring excessive costs and complexity (if the voltage is too high). DC power is less well suited to systems like this proposed lunar grid expansion featuring many different voltage levels because each unique transition between voltage levels requires a new converter design, whereas AC only requires a new transformer design. Beyond showing general trends and making a case for AC, the studies presented here also show a procedure that can be used to select voltages for the expanded lunar grid. Note that if the 1 kHz transmission frequency is used for the expanded scale lunar grid, measures may need to be taken to minimize possible propagation or voltage angle issues that may not occur with lower frequency power transmission. Future work should revisit the grid frequency design space prior to planning expanded operations.

IV. Conclusions

This paper presents trade studies to explore the design space for the lunar grid. Findings include the fact that DC grids tend to be less massive than three-phase AC for the same voltage, especially for higher voltage designs. This is due to the faster increase in cable insulation mass with AC compared to DC. Another is that though AC grids tend to be heavier for the same voltage compared to DC, currently available rad-hard power switches are only capable of up to 300 V (after derating), and this limits possible DC grid voltages to about 1.5 kV. This is because as the number of series stages increases, the reliability of the overall converter decreases. Large number of stages (5+) are required to go beyond 1.5 kV, which poses reliability concerns. AC grids with high voltages can be created using DC/AC converters with a single series stage. This is because with AC, transformers can be used to transform from the 100s of volts single stage level to any desired higher voltage level. The ability to use transformers also means AC grids are more extensible, in that transformers can be designed and added to enable new arbitrary voltage levels for additional new transmission or distribution systems. These facts led to the selection of a 3 kVAC grid design, because 3 kV was the minimum mass solution identified in the trade studies. Beyond this, a line frequency of 1 kHz was selected because this frequency resulted in reduced grid converter magnetics mass. Higher frequencies were not considered, as reactive impedance and skin effect begin to become issues in an Artemis scale system beyond 1 kHz. This grid design solution will inform NASA's efforts to develop planetary surface power grid interface specifications and a reference design for a grid-to-120 VDC interface converter. This paper also presents a grid voltage selection study for a hypothetical expansion of the lunar grid beyond Artemis. This expansion adds an additional habitat as well as in-space manufacturing and MW level solar power generation. The study highlights the need for voltage levels in the 10s of kV up to 100 kV range as the grid expands to a multi-MW level over 10s of km.

References

[1] NASA, "Artemis Program," [Online]. Available: https://www.nasa.gov/artemisprogram. [Accessed 21 August 2022].

[2] L. B. Gordon, "Electrical Transmission on the Lunar Surface," NASA Contractor Report, NASA/CR-2001-210759/PT1, 2001.

[3] T. Kerslake, "Lunar Surface-to-Surface Power Transfer," NASA, NASA Technical Memorandum, NASA/TM—2007-21504, 2007.

[4] B. E. Robertson, J. McNabb, M. R. Rines, D. N. Mavris, D. Stanley, M. Gupta and C. and Taylor, "A Comprehensive Study on the Effectiveness of Power Distribution Systems for Deployment on the Lunar Surface," in *AIAA ASCEND*, Las Vegas, NV, 2021.

[5] A. Colozza, "Small Lunar Base Camp and In Situ Resource Utilization Oxygen Production Facility Power System Comparison," NASA Contractor Report, CR E-19754, Available online: https://ntrs.nasa.gov/citations/20200001622 (accessed on 10 January 2021), 2020.

[6] P. Hanlon, G. L. Thomas, J. Csank and D. J. Sadey, "A Tool for Modeling and Analysis of Electrified Aircraft Power Systems," in *AIAA Propulsion and Energy 2019 Forum*, Indianapolis, IN, 2019.

[7] NASA, "Electrical Power System - Sizing and Analysis Tool (EPS-SAT) (LEW-20017-1)," [Online]. Available: https://software.nasa.gov/software/LEW-19857-1. [Accessed 27 09 2022].

[8] E. Rosa, "The Self and Mutual Inductances of Linear Conductors," Bulletin of the Bureau of Standards, Vol. 4, No. 2, Washington, 1907.

[9] J. Riba, "Analysis of Formulas to Calculate the AC Resistance of Different Conductors' Configurations," *Elect. Power Syst. Res.,* vol. 127, pp. 93-100, 2015.

[10] K. Metcalf, "Power Management and Distribution (PMAD) Model Development: Final Report," November 2011. [Online]. Available: https://ntrs.nasa.gov/citations/20110023763. [Accessed 5 July 2021].

[11] "NASA Identifies Candidate Regions for Landing Next Americans on Moon," NASA, [Online]. Available: https://www.nasa.gov/press-release/nasa-identifies-candidate-regions-for-landing-next-americans-on-moon.

[12] E. Sefton-Nash, M. Siegler and D. Paige, "Thermal Extremes in Permanently Shadowed Regions at the Lunar South Pole," in *Proceedings of the 44th Lunar and Planetary Science Conference*, 2013.

[13] A. R. Vasavadaa, D. A. Paige and S. E. Wood, "Near-Surface Temperatures on Mercury and the Moon and the Stability of Polar Ice Deposits," *Icarus 141 (2),* pp. 179-193, 1999.